

# Roles of G $\beta\gamma$ in membrane recruitment and activation of p110 $\gamma$ /p101 phosphoinositide 3-kinase $\gamma$

Carsten Brock,<sup>1,2,4</sup> Michael Schaefer,<sup>2</sup> H. Peter Reusch,<sup>3</sup> Cornelia Czupalla,<sup>1,2</sup> Manuela Michalke,<sup>2</sup> Karsten Spicher,<sup>2</sup> Günter Schultz,<sup>2</sup> and Bernd Nürnberg<sup>1,2</sup>

<sup>1</sup>Institut für Physiologische Chemie II, Klinikum der Heinrich-Heine-Universität, 40225 Düsseldorf, Germany

<sup>2</sup>Institut für Pharmakologie, <sup>3</sup>Institut für Klinische Pharmakologie und Toxikologie, and <sup>4</sup>Fachbereich Biologie, Chemie, Pharmazie, Freie Universität Berlin, 14195 Berlin, Germany

Receptor-regulated class I phosphoinositide 3-kinases (PI3K) phosphorylate the membrane lipid phosphatidylinositol (PtdIns)-4,5-P<sub>2</sub> to PtdIns-3,4,5-P<sub>3</sub>. This, in turn, recruits and activates cytosolic effectors with PtdIns-3,4,5-P<sub>3</sub>-binding pleckstrin homology (PH) domains, thereby controlling important cellular functions such as proliferation, survival, or chemotaxis. The class I<sub>B</sub> p110 $\gamma$ /p101 PI3K $\gamma$  is activated by G $\beta\gamma$  on stimulation of G protein-coupled receptors. It is currently unknown whether in living cells G $\beta\gamma$  acts as a membrane anchor or an allosteric activator of PI3K $\gamma$ , and which role its noncatalytic p101 subunit plays in its activation by G $\beta\gamma$ . Using GFP-tagged PI3K $\gamma$  subunits expressed in HEK cells, we show that G $\beta\gamma$

recruits the enzyme from the cytosol to the membrane by interaction with its p101 subunit. Accordingly, p101 was found to be required for G protein-mediated activation of PI3K $\gamma$  in living cells, as assessed by use of GFP-tagged PtdIns-3,4,5-P<sub>3</sub>-binding PH domains. Furthermore, membrane-targeted p110 $\gamma$  displayed basal enzymatic activity, but was further stimulated by G $\beta\gamma$ , even in the absence of p101. Therefore, we conclude that in vivo, G $\beta\gamma$  activates PI3K $\gamma$  by a mechanism assigning specific roles for both PI3K $\gamma$  subunits, i.e., membrane recruitment is mediated via the noncatalytic p101 subunit, and direct stimulation of G $\beta\gamma$  with p110 $\gamma$  contributes to activation of PI3K $\gamma$ .

## Introduction

Phosphoinositide 3-kinases (PI3Ks)\* phosphorylate the D3 position of the inositol ring of phosphoinositides, thereby generating intracellular signaling molecules (Stephens et al., 1993; Fruman et al., 1998). These phospholipids, i.e., phosphatidylinositol (PtdIns)-3-P, PtdIns-3,4-P<sub>2</sub>, and PtdIns-3,4,5-P<sub>3</sub>, have been implicated in cellular functions including chemotaxis, differentiation, glucose homeostasis, proliferation, survival, and trafficking (Vanhaesebroeck et al., 2001; Cantley, 2002). They transmit signals by recruiting effector molecules that possess specific lipid-binding domains. FYVE domains

and PX domains bind to PtdIns-3-P with high affinity, whereas a subgroup of pleckstrin homology (PH) domains, containing a highly basic motif, preferentially binds PtdIns-3,4-P<sub>2</sub> and PtdIns-3,4,5-P<sub>3</sub> (Hurley and Misra, 2000; Simonsen et al., 2001; Wishart et al., 2001).

PtdIns-3,4,5-P<sub>3</sub> represents the major product of class I PI3Ks in vivo. These lipid kinases are under tight control of cell surface receptors, including receptor tyrosine kinases (RTK) or G protein-coupled receptors (GPCR; Katso et al., 2001). All class I members are heterodimers consisting of a p110 catalytic and a p85- or p101-type noncatalytic subunit. The class I<sub>A</sub> p110 isoforms  $\alpha$ ,  $\beta$ , and  $\delta$  form a complex with p85 adaptor subunits, whereas the only class I<sub>B</sub> member (p110 $\gamma$ ) is associated with a p101 noncatalytic subunit. The p85 subunit binds to tyrosine-phosphorylated RTKs. This interaction has two consequences resulting in activation of the PI3K. First, the cytosolic enzyme translocates to the inner leaflet of the plasma membrane, giving p110 access to its lipid substrate (Gillham et al., 1999). Second, the interaction with the tyrosine-phosphorylated receptor induces a conformational change of p85 that results in disinhibition of p110 enzymatic activity (Yu et al., 1998). Because the p85 regulatory subunit inhibits the p110 catalytic subunit, it is feasible that

Address correspondence to Bernd Nürnberg, Institut für Physiologische Chemie II, Klinikum der Heinrich-Heine-Universität, Universitätsstr. 1, Gebäude 22.03, 40 225 Düsseldorf. Tel.: 49-211-811-2724. Fax: 49-211-811-2726. E-mail: bernd.nuernberg@uni-duesseldorf.de

\*Abbreviations used in this paper: Btk, Bruton's tyrosine kinase; fMLP, formyl-methionyl-leucyl-phenylalanine; FRET, fluorescence resonance energy transfer; GPCR, G protein-coupled receptor; GRP1, general receptor for phosphoinositides-1; HEK, human embryonic kidney; PH, pleckstrin homology; PtdIns, phosphatidylinositol; PI3K, phosphoinositide 3-kinase; PTX, pertussis toxin; RTK, receptor tyrosine kinase; VSM, vascular smooth muscle.

Key words: G protein; fluorescence imaging; phosphoinositide 3-kinase; FRET; PH domain

constitutively membrane-associated class I<sub>A</sub> p110 mutants trigger downstream responses characteristic of growth factor action (Klippel et al., 1996).

Similar to class I<sub>A</sub> PI3Ks, unstimulated PI3K $\gamma$  is predominantly localized in the cytosol, whereas GPCRs induced an increase of PI3K $\gamma$  in the membrane fraction (Al-Aoukaty et al., 1999; Naccache et al., 2000). GPCRs activate PI3K $\gamma$  through direct interaction with G $\beta\gamma$ , whereas a stimulation by G $\alpha$  is quantitatively less important (Stoyanov et al., 1995; Stephens et al., 1997; Leopoldt et al., 1998). However, little is known about the activating mechanism, e.g., it remains elusive whether G $\beta\gamma$  functions as a membrane anchor or an allosteric regulator of PI3K $\gamma$ . Although the p101 subunit has been proposed to act as an indispensable adaptor linking G $\beta\gamma$  with p110 $\gamma$  (Stephens et al., 1997), *in vitro* studies have suggested that p101 is not mandatory for G $\beta\gamma$ -induced stimulation of PI3K $\gamma$  (Stoyanov et al., 1995). Moreover, a direct interaction of G $\beta\gamma$  with NH<sub>2</sub>- and COOH-terminal regions of p110 $\gamma$  has been demonstrated (Leopoldt et al., 1998). Further support for a direct interaction of G $\beta\gamma$  with the p110 catalytic subunit came from the observation that the p110 $\beta$  isoform can also be stimulated by G $\beta\gamma$ , regardless of whether p85 is present or not (Kurosu et al., 1997; Maier et al., 1999, 2000). Nevertheless, the noncatalytic p101 subunit of PI3K $\gamma$  binds tightly to G $\beta\gamma$ , suggesting specific roles in G protein-induced regulation of this lipid kinase. For instance, *in vitro* studies showed that G $\beta\gamma$ -stimulated p110 $\gamma$  potently produced PtdIns-3-P, whereas the G $\beta\gamma$ -activated heterodimeric p110 $\gamma$ /p101 counterpart potently catalyzed the formation of PtdIns-3,4,5-P<sub>3</sub> (Maier et al., 1999). This suggests that p101 may affect the interaction of G $\beta\gamma$ -stimulated p110 $\gamma$  with the lipid interface.

Therefore, the exact roles of G $\beta\gamma$  and PI3K $\gamma$  subunits in G protein-induced activation of PI3K $\gamma$  in living cells remain unclear. Hence, we asked whether G $\beta\gamma$  functions as a membrane anchor and/or allosteric activator, and whether p101 is required for proper function of p110 $\gamma$  *in vivo*. To tackle these questions, we examined cellular events leading to activation of PI3K $\gamma$  using fluorescent fusion proteins in living cells.

## Results

### Characterization of fluorescent PI3K fusion proteins

To visualize PI3K $\gamma$  subunits *in vivo*, we generated constructs encoding p110 $\gamma$  and p101 fused to YFP or CFP (Fig. 1 A). Their expression in human embryonic kidney (HEK) 293 cells was verified by immunoblot analysis using an antibody against GFP (Fig. 1 B). The catalytic activity and G $\beta\gamma$  sensitivity of PI3K $\gamma$  fusion proteins was confirmed by *in vitro* lipid kinase assays after immunoprecipitation with an mAb recognizing only intact p110 $\gamma$  (Fig. 1 C). Precipitates from vector-transfected control cells neither exhibited p110 $\gamma$  immunoreactivity nor lipid kinase activity. These results demonstrate that YFP-fused p110 $\gamma$  or p101 retain essential functions of the wild-type PI3K $\gamma$ .

### Subcellular distribution of PI3K $\gamma$ subunits and instability of monomeric p101

Next, we examined the subcellular distribution of the YFP-tagged PI3K $\gamma$  subunits in living cells by confocal laser scan-

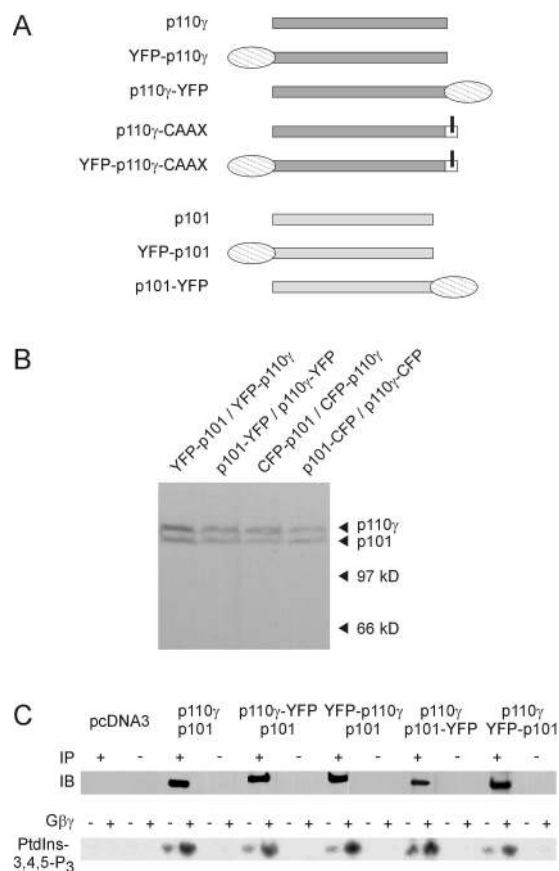


**Figure 1. Construction and characterization of fluorescent PI3K $\gamma$  fusion proteins.** (A) Schematic representation of the wild-type, fluorescent, and membrane-targeted PI3K $\gamma$  subunits. A YFP (or CFP) tag was fused to either the NH<sub>2</sub>- or the COOH terminus of p110 $\gamma$  and p101. The p110 $\gamma$ -CAAX fusion protein contains an isoprenylation motif (bars for lipid modifications). (B) Differently fluorescence-tagged PI3K $\gamma$  subunits were coexpressed in HEK cells, and cell lysates were subjected to SDS-PAGE followed by immunoblotting with a GFP-specific antibody. (C) Catalytic activity of fluorescent PI3K $\gamma$  fusion proteins. HEK cells were transfected with the indicated plasmids. Lysates were subjected to immunoprecipitation (IP) with (+) or without (-) an anti-p110 $\gamma$  antibody. Immunoprecipitation was controlled by immunoblotting (IB) with another anti-p110 $\gamma$  antibody. Shown are chemiluminescence images (top panels). Immunoprecipitates were assayed for *in vitro* PI3K activity in the absence or presence of 120 nM G $\beta\gamma$  using PtdIns-4,5-P<sub>2</sub>-containing lipid vesicles and  $\gamma$ [<sup>32</sup>P]ATP as substrates. Depicted are autoradiographs of the generated <sup>32</sup>P-PtdIns-3,4,5-P<sub>3</sub> (bottom panels).

ning microscopy. Although YFP was uniformly distributed inside HEK cells (unpublished data), fluorescence signals from YFP fused to the NH<sub>2</sub> or COOH termini of p110 $\gamma$  were only detected in the cytosolic compartment (Fig. 2 A, top). However, a small fraction of the YFP-fused p110 $\gamma$  was also detected in the nucleus when coexpressed with wild-type p101 (Fig. 2 B, top). The same distribution was seen for YFP-tagged p101 coexpressed with wild-type p110 $\gamma$  (Fig. 2 B, bottom). Thus, fluorescent PI3K $\gamma$  subunits form heterodimers (see next section), present in the cytosol and nucleus of HEK cells, whereas distribution of the p110 $\gamma$  subunit alone seems restricted to the cytosol. Interestingly, YFP-fused p101 alone showed a predominant nuclear local-

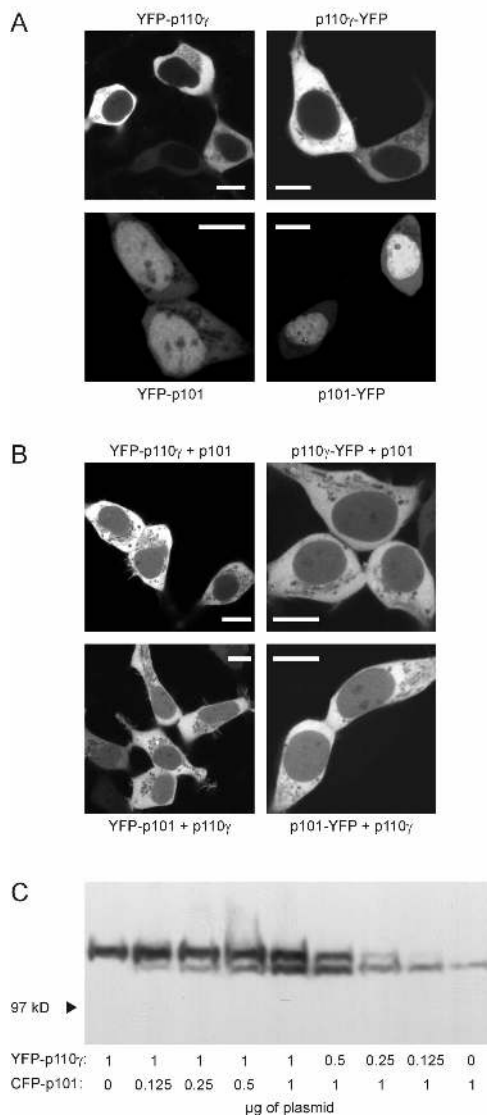


**Figure 2. Expression and subcellular distribution of fluorescent p110 $\gamma$  and p101 in HEK cells.** (A) Cells were transfected with plasmids for YFP-tagged single PI3K $\gamma$  subunits as indicated. Images were taken by confocal laser scanning microscopy. Images of typical cells are shown. White bars indicate a 10- $\mu$ m scale. (B) Cells were cotransfected with both p110 $\gamma$  and p101. Only one subunit was fused to YFP as indicated. (C) Cells were transfected with plasmids encoding fluorescent p110 $\gamma$  and p101 at different ratios. The total amount of transfected cDNA was kept constant by the addition of pcDNA3. Equal amounts of whole-cell lysates were subjected to SDS-PAGE followed by immunoblotting with an anti-GFP antibody.

ization with a significantly lower overall fluorescence intensity (Fig. 2 A, bottom).

To explore the possibility that expression levels of p101 could depend on the coexpression of p110 $\gamma$ , we transfected HEK cells with different ratios of plasmids encoding fluorescent p110 $\gamma$  or p101 and analyzed total cell lysates by immunoblotting using an anti-GFP antibody (Fig. 2 C). The expression level of p110 $\gamma$  correlated with the amount of the p110 $\gamma$  (but not the p101) plasmid. In contrast, the expression level of p101 was also dependent on the amount of the p110 $\gamma$  plasmid. Hence, the stability of p101 depends on the

coexpression of p110 $\gamma$ , but not vice versa. The poor cytosolic fluorescence of YFP-tagged p101 in the absence of p110 $\gamma$  may thus be explained by cytosolic degradation of monomeric p101.

### In vivo dimerization of PI3K $\gamma$ subunits

To directly demonstrate heterodimerization of PI3K $\gamma$  subunits in living cells, we used fluorescence resonance energy transfer (FRET). FRET between two fluorophores, e.g., CFP and YFP, is restricted to distances of <100 Å, and therefore, provides direct evidence for a protein–protein interaction (Teruel and Meyer, 2000). We coexpressed CFP- and YFP-tagged PI3K $\gamma$  subunits and determined FRET by following the donor (CFP) recovery during acceptor (YFP) bleach (Fig. 3 A). All combinations showed significant FRET, although quantitative differences were evident.

Because FRET efficiency is a function of the distance between two fluorophores, quantitative differences may represent different distances of the fluorescent tags fused to the NH<sub>2</sub> or COOH termini of p101 and p110 $\gamma$  in a particular combination. However, the different FRET efficiencies may

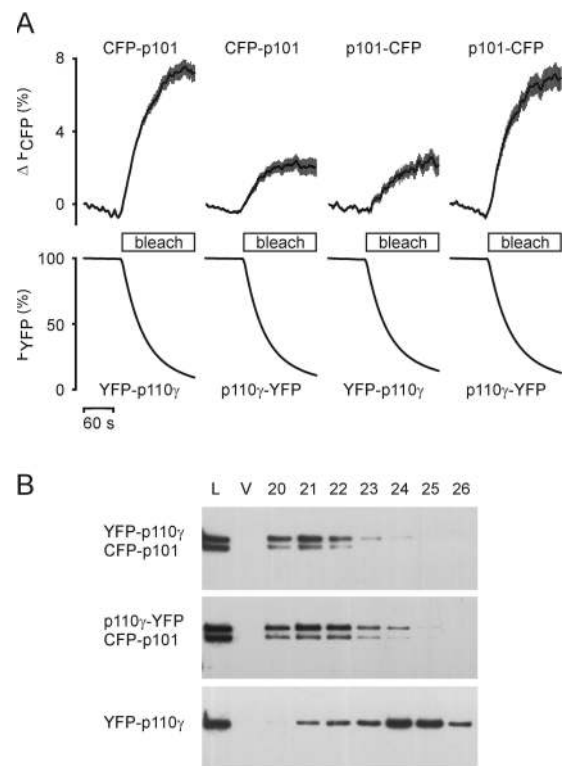
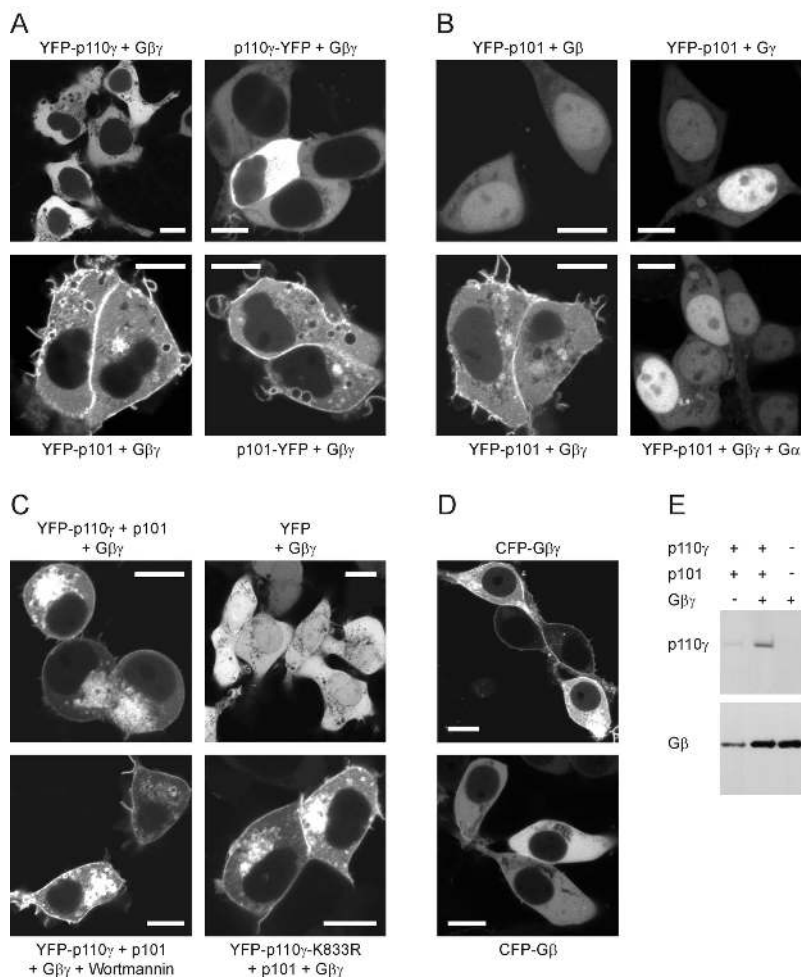


**Figure 3. Dimerization of p110 $\gamma$  and p101.** (A) HEK cells were cotransfected with plasmids encoding NH<sub>2</sub>- or COOH-terminally YFP-tagged p110 $\gamma$  and NH<sub>2</sub>- or COOH-terminally CFP-tagged p101 in different combinations. FRET was measured in vivo. An increase in CFP (donor) fluorescence during YFP (acceptor) bleach indicates FRET between fluorescent PI3K $\gamma$  subunits. The depicted data represent means  $\pm$  SEM of at least 18 single cells in three independent transfection experiments. (B) HEK cells were transfected with the indicated plasmids. Cytosols were prepared and subjected to gel filtration. The elution profiles were analyzed by immunoblotting with an anti-GFP antibody (L, load diluted 1:5; V, void volume; 20–26, fraction numbers).

**Figure 4. Membrane recruitment of PI3K $\gamma$  by G $\beta$  $\gamma$ .** The effect of coexpression of G $\beta$  $\gamma$  on the subcellular distribution of p110 $\gamma$ , p101, and heterodimeric PI3K $\gamma$  in HEK cells was analyzed by confocal laser scanning microscopy. Images of typical cells are shown (white bars, 10  $\mu$ m). (A) Coexpression of monomeric PI3K $\gamma$  subunits with G $\beta$  $\gamma$ . (B) Controls; coexpression of YFP-p101 with G $\beta$  $\gamma$ , G $\gamma$  $\gamma$ , G $\beta$  $\gamma$  $\gamma$ , or G $\beta$  $\gamma$  $\gamma$  and the G $\beta$  $\gamma$ -scavenging G $\alpha$  $\gamma$  $\gamma$ . (C) Coexpression of heterodimeric PI3K $\gamma$  with G $\beta$  $\gamma$ . Note the round shape of the cells. Controls; coexpression of G $\beta$  $\gamma$  with YFP or with kinase-deficient YFP-p110 $\gamma$ -K833R and p101; effect of 100 nM wortmannin. (D) Subcellular localization of G $\beta$  $\gamma$ . Cells were transfected with a plasmid encoding CFP-tagged G $\beta$  $\gamma$  alone or together with the G $\gamma$  $\gamma$  plasmid. (E) Immunoblot analysis of membrane fractions. HEK cells were transfected with the plasmids encoding PI3K $\gamma$ , G $\beta$  $\gamma$ , or both together. To avoid rounding and detachment of the cells, the kinase-deficient mutant YFP-p110 $\gamma$ -K833R was used. Membrane fractions were prepared and analyzed by immunoblotting with anti-p110 $\gamma$  and anti-G $\beta$  antibodies.



also reflect different degrees of heterodimerization. To exclude the latter, we analyzed heterodimerization of different p101/p110 $\gamma$  combinations by size-exclusion chromatography (Fig. 3 B). The elution profile of YFP-p110 $\gamma$  (Fig. 3 B, bottom) was completely shifted to earlier fractions on coexpression with CFP-p101 (Fig. 3 B, top), indicating a high degree of heterodimerization. A similar elution profile was found for p110 $\gamma$ -YFP + CFP-p101 (Fig. 3 B, middle), albeit a lower FRET efficiency was detected for this combination. Hence, the different FRET efficiencies observed are not due to different degrees of dimerization, but likely reflect different distances of the fluorescent tags in the p101/p110 $\gamma$  heterodimer. Thus, their two NH $_2$  termini as well as their two COOH termini are in close proximity, whereas the NH $_2$  terminus of each subunit is relatively far from the COOH terminus of the other.

#### G $\beta$ $\gamma$ dimers recruit PI3K $\gamma$ to membranes via the p101 subunit

Current concepts of PI3K activation are based on the recruitment of the cytosolic lipid kinase to the plasma membrane (Klippel et al., 1996). In the case of PI3K $\gamma$ , the major stimulus is assumed to be G $\beta$  $\gamma$ , which is membrane-bound and has been shown to directly bind to both kinase subunits under in vitro conditions (Stephens et al., 1997; Maier et al., 1999). Therefore, we asked whether overex-

pression of free G $\beta$  $\gamma$  directs YFP-fused PI3K $\gamma$  subunits to the cell membrane in vivo. Surprisingly, p110 $\gamma$  was not membrane-localized in the presence of coexpressed G $\beta$  $\gamma$  in HEK cells (Fig. 4 A, top). In contrast, G $\beta$  $\gamma$  recruited p101 to the membrane, resulting in accumulation of NH $_2$ - or COOH-terminally YFP-tagged p101 at both plasma- and endomembranes (Fig. 4 A, bottom, and Fig. 4 B). This corresponds to the subcellular distribution of overexpressed G $\beta$  $\gamma$  dimers (see below), suggesting that p101 interacted with membrane-bound G $\beta$  $\gamma$ .

Next, we examined the subcellular localization of p110 $\gamma$ /p101 heterodimers in the presence of free G $\beta$  $\gamma$ . When coexpressed with p101 and G $\beta$  $\gamma$ , the p110 $\gamma$  fluorescent signal was at, or close to, plasma and endosomal membranes of HEK cells (Fig. 4 C, top). The same picture emerged when the YFP-tag was fused to p101 (unpublished data). Correspondingly, CFP-tagged G $\beta$  $\gamma$  coexpressed with G $\gamma$  $\gamma$  exhibited a similar subcellular distribution like fluorescent heterodimeric PI3K $\gamma$  (compare Figs. 4 C and 4 D), and immunoblotting of membrane-derived proteins confirmed an enrichment of PI3K $\gamma$  in the membrane compartment after overexpression of G $\beta$  $\gamma$  (Fig. 4 E). Together, these data imply that G $\beta$  $\gamma$  directs cytosolic PI3K $\gamma$  to the membrane via interaction with p101.

Interestingly, coexpression of heterodimeric PI3K $\gamma$  together with G $\beta$  $\gamma$  produced a rounded morphology and de-

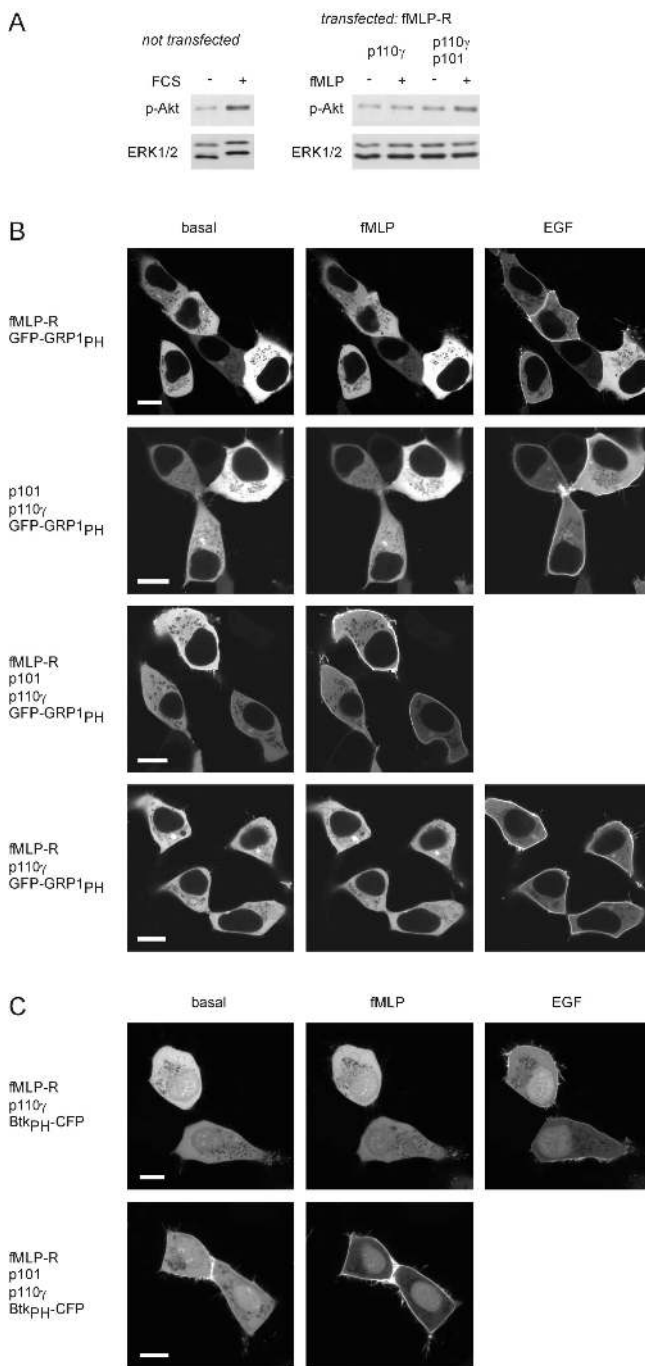


**Figure 5. Activation of PI3K $\gamma$  by a G protein-coupled receptor.** (A) Akt phosphorylation. Whole-cell lysates were analyzed by immunoblotting using an antibody that specifically recognizes the phosphorylated form of Akt. Equal loading was shown by using an anti-ERK antibody. Left; FCS-induced Akt phosphorylation in untransfected HEK cells. Right; fMLP-induced Akt phosphorylation in cells expressing the fMLP receptor and only the catalytic (p110 $\gamma$ ) or both PI3K $\gamma$  subunits. (B) Membrane recruitment of the PtdIns-3,4,5- $P_3$ -binding PH domain of GRP1. HEK 293 cells were transfected with plasmids encoding the PH domain of GRP1 fused to GFP (GFP-GRP1<sub>PH</sub>), and the human fMLP receptor (fMLP-R), p110 $\gamma$ , and p101 in different combinations. The localization of the GFP-GRP1<sub>PH</sub> was monitored before and after the addition of 1  $\mu$ M fMLP and 100 ng/ml EGF (added 8 min later) by confocal laser scanning microscopy. Pictures were taken 4 min after addition of either agonist. Images of typical experiments are shown (white

bars, 10  $\mu$ m). (C) Membrane recruitment of the PtdIns-3,4,5- $P_3$ -binding PH domain of Btk. Instead of GFP-GRP1<sub>PH</sub>, the PH domain of Btk fused to CFP (Btk<sub>PH</sub>-CFP) was used as a PtdIns-3,4,5- $P_3$  sensor.

tachment of the cells (Fig. 4 C). This morphological change was reversed by treatment with 100 nM of the PI3K inhibitor wortmannin in approximately half of the cells within 30 min, and not seen when a kinase-deficient YFP-p110 $\gamma$ -K833R mutant was used (Fig. 4 C). Hence, the morphological change was related to the enzymatic activity of PI3K $\gamma$  stimulated by the coexpressed G $\beta\gamma$ .

### p101 is required for G protein-mediated activation of p110 $\gamma$ in vivo

Because changes in morphology are not a very reliable measure of PI3K activity, we examined phosphorylation of endogenous protein kinase B (PKB or Akt) as an established PI3K-specific read-out system. To avoid detachment of the cells as a consequence of constitutive PI3K $\gamma$  stimulation by overexpressed G $\beta\gamma$ , we transiently stimulated the heterologously expressed G $\beta\gamma$ -coupled formyl-methionyl-leucyl-phenylalanine (fMLP) receptor, which is known to activate PI3K $\gamma$  (Stephens et al., 1993). Stimulation with fMLP induced Akt phosphorylation in HEK cells in the same range as with FCS (Fig. 5 A). However, Akt phosphorylation was only seen when the receptor was coexpressed with both PI3K $\gamma$  subunits, and not with p110 $\gamma$  alone. These data imply that p101 is required for GPCR-induced activation of PI3K $\gamma$  in vivo.

To measure PI3K $\gamma$  activity by a complementary experimental approach, the effects of fMLP receptor stimulation on the subcellular distribution of GFP-GRP1<sub>PH</sub> fusion proteins were examined. Recruitment of the GFP-labeled PH domain of general receptor for phosphoinositides-1 (GRP1), a PI3K-activated exchange factor for ADP-ribosylation factors (Lietzke et al., 2000), has been applied to detect formation of PtdIns-3,4,5- $P_3$  with high affinity and selectivity (Gray et al., 1999; Balla et al., 2000). fMLP stimulation had no effect on the subcellular distribution of GFP-GRP1<sub>PH</sub> in HEK cells expressing either the receptor or PI3K $\gamma$  alone (Fig. 5 B, top two panels), whereas subsequent stimulation with EGF induced a rapid membrane recruitment of the PtdIns-3,4,5- $P_3$  sensor, presumably through activation of an endogenously expressed RTK-sensitive class I<sub>A</sub> PI3K. In cells coexpressing the fMLP receptor and heterodimeric PI3K $\gamma$ , fMLP stimulation induced a rapid membrane translocation of GFP-GRP1<sub>PH</sub> (Fig. 5 B, third panel), indicating that this effect indeed reflects fMLP receptor-mediated stimulation of PI3K $\gamma$ . Accordingly, the fMLP-induced effect was sensitive to pretreatment with pertussis toxin (PTX; unpublished data). Interestingly, a slight basal membrane localization of GFP-GRP1<sub>PH</sub> was visible in the cells coexpressing heterodimeric PI3K $\gamma$  and the fMLP receptor even in the absence of agonist (Fig. 5 B, third panel). Because this was not seen after PTX treatment (unpublished data) or in cells omitting the receptor (Fig. 5 B, second panel), it most likely reflected a constitutively active fMLP receptor.

Translocation of an isolated PH domain in single cells may be a more sensitive read-out for PtdIns-3,4,5- $P_3$  production than the Akt phosphorylation assay. Hence, we used

bars, 10  $\mu$ m). (C) Membrane recruitment of the PtdIns-3,4,5- $P_3$ -binding PH domain of Btk. Instead of GFP-GRP1<sub>PH</sub>, the PH domain of Btk fused to CFP (Btk<sub>PH</sub>-CFP) was used as a PtdIns-3,4,5- $P_3$  sensor.

the GFP-GRP1<sub>PH</sub> translocation approach to reexamine the requirement of p101 for receptor-induced PI3K $\gamma$  activation (Fig. 5 A). Nevertheless, an fMLP-induced membrane recruitment of GFP-GRP1<sub>PH</sub> in cells coexpressing the receptor and p110 $\gamma$  (but not p101) was not visible (Fig. 5 B, fourth panel). This finding confirms that the noncatalytic p101 subunit is required for GPCR-mediated stimulation of PI3K $\gamma$  in living cells.

To further strengthen the findings, we replaced GFP-GRP1<sub>PH</sub> by the GFP-fused PH domain of Bruton's tyrosine kinase (Btk<sub>PH</sub>), which has also been described to bind Ptd-Ins-3,4,5-P<sub>3</sub> with high specificity and affinity (Várnai et al., 1999). As expected, fluorescent Btk<sub>PH</sub> was distributed equally between cytosol and nucleus in HEK cells (Fig. 5 C). However, cells coexpressing the receptor and both PI3K $\gamma$  subunits exhibited a slight basal membrane localization of Btk<sub>PH</sub>-CFP followed by a prominent translocation from the cytosol to the membrane on exposure to fMLP. Similar to GFP-GRP1<sub>PH</sub>, no fMLP-induced redistribution of Btk<sub>PH</sub>-CFP was seen in the absence of p101.

### Activation of a membrane-targeted p110 $\gamma$ -CAAX in vivo

The presented data suggest that in living cells, p101 is an indispensable adaptor for GPCR-induced translocation and activation of class I<sub>B</sub> PI3K $\gamma$ , which is equivalent to the role of p85 in RTK-induced class I<sub>A</sub> PI3K activation. Vice versa, G $\beta\gamma$  behaves as a membrane anchor recruiting PI3K $\gamma$  through association with p101. So far, these experiments did not clarify whether membrane recruitment itself is sufficient for activation of the enzyme or whether additional allosteric stimulation is required. To tackle this question, we generated p110 $\gamma$  mutants containing a COOH-terminal isoprenylation signal, i.e., a CAAX-box motif, which constitutively localizes p110 $\gamma$  to the plasma membrane. p110 $\gamma$ -CAAX accumulated

at the plasma membrane of HEK cells, and was able to complex with p101 (Fig. 6, top). Coexpression of G $\beta\gamma$  together with YFP-p110 $\gamma$ -CAAX increased not only fluorescent staining of endomembranes, but also produced a wortmannin-sensitive rounding of the cells (Fig. 6, bottom) even in the absence of p101 (not depicted), which was similar to the effect after coexpression of G $\beta\gamma$  with p110 $\gamma$ /p101 dimers (see Fig. 4 C). These observations imply that membrane-bound PI3K $\gamma$  is not fully active, but can be further activated by G $\beta\gamma$ .

To substantiate this assumption, we analyzed the subcellular redistribution of GFP-GRP1<sub>PH</sub> in HEK cells coexpressing membrane-targeted p110 $\gamma$ -CAAX, p101 and the fMLP receptor in various combinations (Fig. 7 A). A slight basal membrane localization of the fluorescent PH domain was evident on coexpression with p110 $\gamma$ -CAAX (Fig. 7 A, top panel) indicating an elevated PtdIns-3,4,5-P<sub>3</sub> level. The same picture emerged when p101 was present in the panel of transfected plasmids (Fig. 7 A, second panel). On coexpression of the receptor, fMLP induced a significant additional translocation of GFP-GRP1<sub>PH</sub> from the cytosol to the membrane (Fig. 7 A, third and fourth panel) indicating additional stimulation of the membrane-bound lipid kinase. Interestingly, the effect was similar irrespective of whether p101 was present or not, suggesting direct activation of monomeric p110 $\gamma$ . PTX sensitivity confirmed that fMLP-induced activation of p110 $\gamma$ -CAAX was mediated by G<sub>i</sub> proteins (unpublished data). Because G $\beta\gamma$  can activate Ras, which in turn may activate p110 $\gamma$ , one may imagine that fMLP-induced, p101-independent stimulation of p110 $\gamma$ -CAAX was mediated by Ras. However, coexpression of dominant-negative Ras N17 had no effect on fMLP-induced p110 $\gamma$ -CAAX stimulation, whereas its inhibitory effect was evident when EGF-induced MAP kinase activation was assessed (Fig. 7 A, bottom panel). In addition, an indirect autocrine stimulatory effect was excluded because supernatants of fMLP-stimulated cells failed to induce GFP-GRP1<sub>PH</sub> translocation in cells omitting fMLP receptors (unpublished data).

By using Btk<sub>PH</sub>-CFP instead of GFP-GRP1<sub>PH</sub> as the Ptd-Ins-3,4,5-P<sub>3</sub> sensor, we confirmed both the basal enzymatic activity and fMLP-induced stimulation of membrane-targeted p110 $\gamma$ -CAAX, regardless of coexpressed p101 (Fig. 7 B). Furthermore, the Akt phosphorylation assay corroborated that p101 was dispensable for GPCR-induced stimulation of membrane-targeted p110 $\gamma$ -CAAX (Fig. 7 C).

Next, we sought to confirm our principal findings using nontransformed cells in primary culture with a higher degree of differentiation than HEK cells. Vascular smooth muscle (VSM) cells were injected with plasmids encoding the fMLP receptor, p101, p110 $\gamma$  or p110 $\gamma$ -CAAX, and GFP-GRP1<sub>PH</sub> in different combinations, and redistribution of the fluorescent PtdIns-3,4,5-P<sub>3</sub> sensor was monitored (Fig. 8). Again, this series of experiments confirmed that p101 is required for GPCR-mediated activation of PI3K $\gamma$  in living cells, whereas membrane-targeted p110 $\gamma$  can be stimulated even in the absence of p101.

## Discussion

PI3K $\gamma$  is a key player in the regulation of leukocyte functions such as chemotaxis and superoxide production (Katso

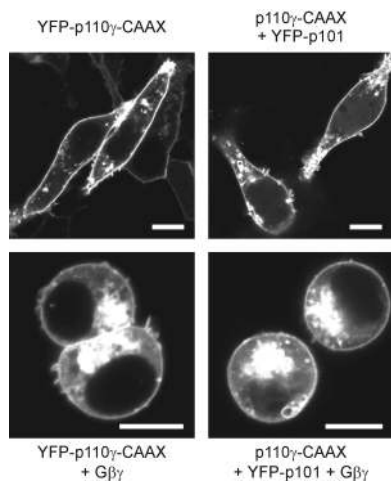


**Figure 6. Characterization of a constitutively membrane-associated p110 $\gamma$ -CAAX.** HEK cells were transfected with the indicated plasmids and analyzed by confocal laser scanning microscopy. Images of typical cells are shown. White bars indicate a 10- $\mu$ m scale. Top panel; Subcellular localization of YFP-p110 $\gamma$ -CAAX (left) or YFP-p101 expressed together with p110 $\gamma$ -CAAX (right). Bottom panel; Coexpression with G $\beta\gamma$ .

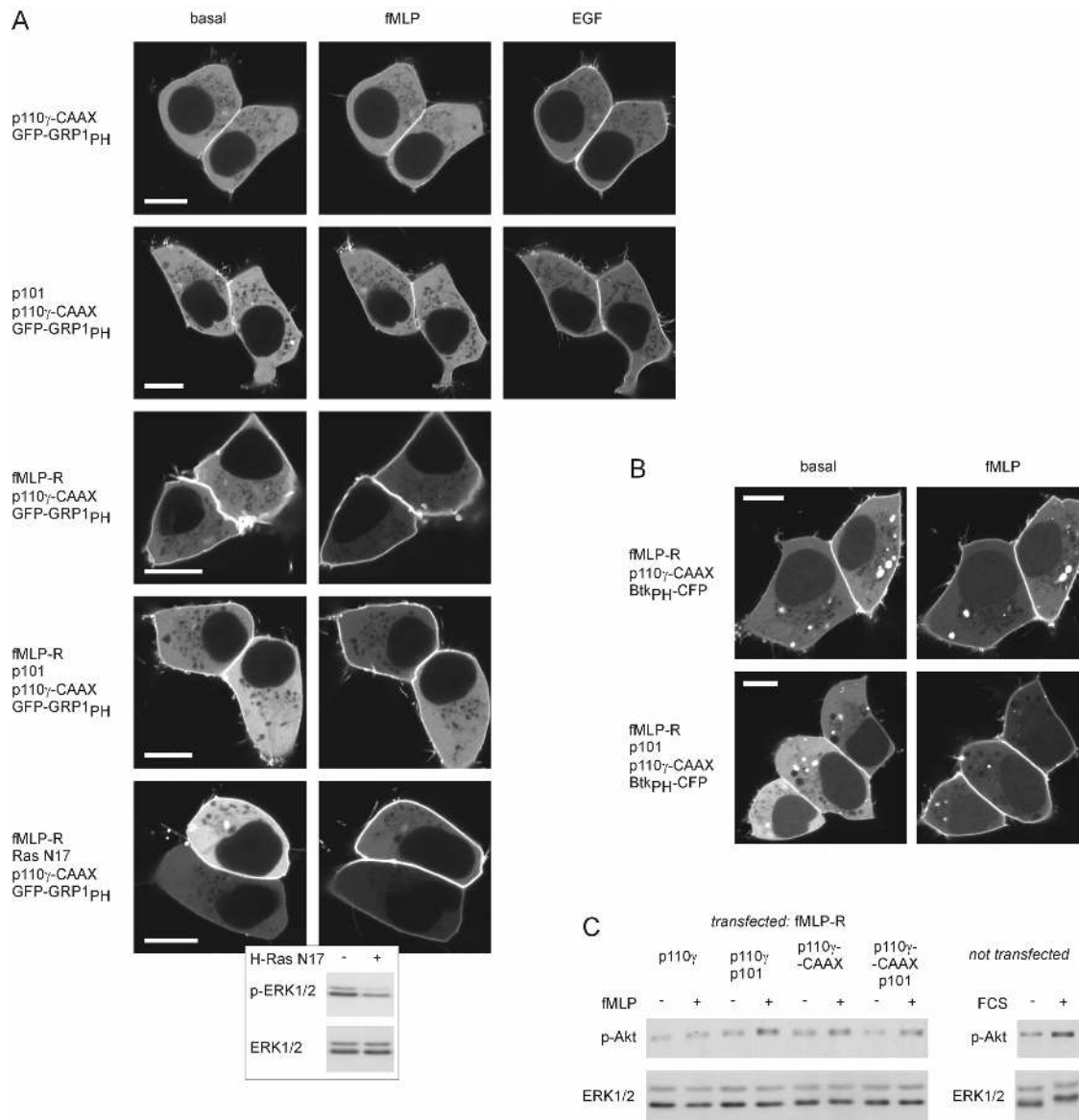


**Figure 7. Activation of a constitutively membrane-associated p110 $\gamma$ -CAAX.** (A) GFP-GRP1<sub>PH</sub> translocation. HEK cells were transfected with plasmids for GFP-GRP1<sub>PH</sub> and p110 $\gamma$ -CAAX, p101, fMLP-R, and dominant-negative Ras N17 in different combinations. Translocation of the PtdIns-3,4,5-P<sub>3</sub>-binding GFP-GRP1<sub>PH</sub> in response to agonist stimulation was monitored as described above (see Fig. 5). White bars indicate a 10- $\mu$ m scale. As a positive control for H-Ras N17, cells were transfected with the H-Ras N17 plasmid (same amount as for the GFP-GRP1<sub>PH</sub> translocation experiment) or empty vector. Cells were stimulated with 10 ng/ml EGF, and whole-cell lysates were analyzed by immunoblotting with an antibody that specifically recognizes the phosphorylated form of ERK (p-ERK). Equal loading was shown using the anti-ERK-antibody. (B) Btk<sub>PH</sub>-CFP translocation. (C) Akt phosphorylation. The experiment shown in Fig. 5 was repeated. In addition, cells were transfected with the plasmid for the membrane-targeted p110 $\gamma$ -CAAX instead of wild-type p110 $\gamma$ .

et al., 2001). To elucidate the mechanism of how G $\beta\gamma$  activates the enzyme *in vivo*, we studied the subcellular localization and translocation of GFP-tagged PI3K $\gamma$  subunits and PH domains in living cells.

A p110 $\gamma$ -GFP construct has been previously reported (Metjian et al., 1999), but data describing a functional interaction of the fusion protein with G proteins are not available. Therefore, we systematically tagged each PI3K $\gamma$  subunit and found heterodimerization, enzymatic activity, and G $\beta\gamma$ -sensitivity of the fusion proteins unaffected by the tags, whereas a GFP-tagged G $\beta$  complexed to G $\gamma$  did not interact with PI3K $\gamma$  (unpublished data). In resting cells, fluorescent PI3K $\gamma$  was predominantly detected in the

cytosol. This resembles the native situation in which the vast majority of the endogenous PI3K $\gamma$  pool has been assigned to the cytosol (Stephens et al., 1994, 1997; Tang and Downes, 1997). Thus, the GFP-tagged proteins are appropriate tools to study the cellular events leading to activation of PI3K $\gamma$ .

Recent analysis of p110 $\gamma$  crystals gave insights into the three-dimensional structure of the catalytic PI3K $\gamma$  subunit (Walker et al., 1999; Pacold et al., 2000). However, the structure of p101 and the molecular determinants for the interaction of both PI3K $\gamma$  subunits are currently unknown. *In vitro* data derived from p101 and p110 $\gamma$  deletion mutants suggest that large areas of p101 may interact with the NH<sub>2</sub>-

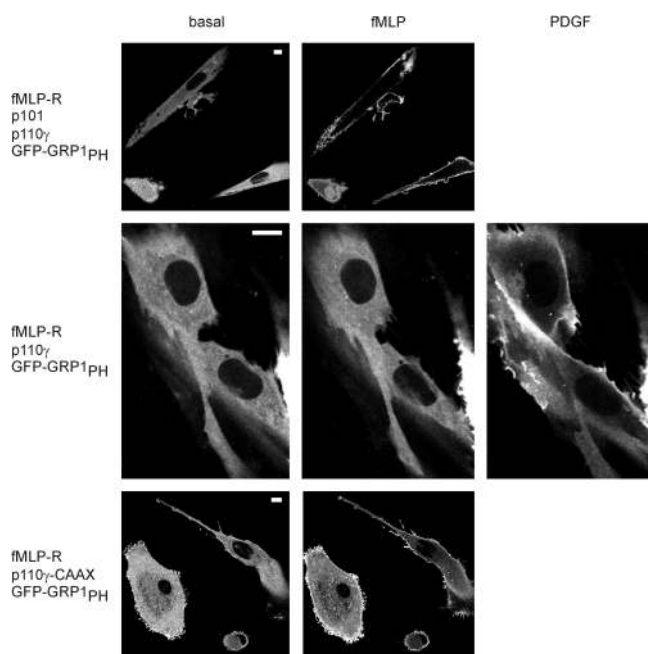


**Figure 8. PI3K $\gamma$ -mediated membrane translocation of GFP-GRP1<sub>PH</sub> in vascular smooth muscle (VSM) cells.** VSM cells were microinjected with plasmids for GFP-GRP1<sub>PH</sub>, fMLP-R, p101, and p110 $\gamma$  or p110 $\gamma$ -CAAX in different combinations. The localization of GFP-GRP1<sub>PH</sub> was monitored before and after the addition of 1  $\mu$ M fMLP (picture taken after 4 min) and 10 ng/ml PDGF-BB (added 12 min later, picture taken after 8 min). White bars indicate a 10- $\mu$ m scale.

terminal side of p110 $\gamma$  (Krugmann et al., 1999). FRET data presented here indicate that NH<sub>2</sub> and both COOH termini of p110 $\gamma$  and p101 are in close proximity. The latter finding is of interest because the p110 $\gamma$  COOH terminus harbors the catalytic domain. Previous data have implied that not only Ras (Pacold et al., 2000), but also G $\beta$  $\gamma$  (Leopoldt et al., 1998) directly interact with the COOH terminus of p110 $\gamma$ . Therefore, interaction of p101 with the catalytic domain of p110 $\gamma$  would be in line with the functional data suggesting

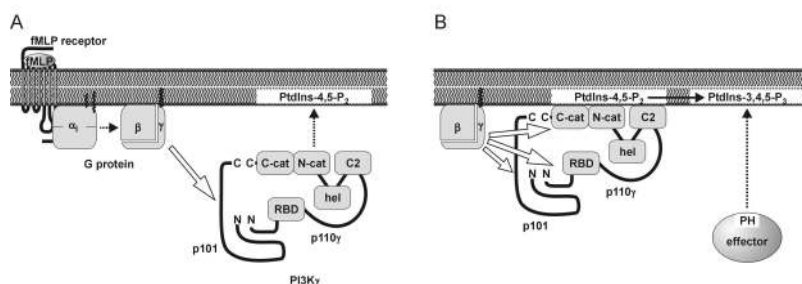
that p101 affects interaction of G $\beta$  $\gamma$ -stimulated p110 $\gamma$  with the lipid interface (Maier et al., 1999).

G $\beta$  $\gamma$  is considered to be the principal, direct stimulus of GPCR-induced PI3K $\gamma$  enzymatic activity. Convincing evidence for this assumption has come from reconstitution of purified proteins, demonstrating that *in vitro*, the enzymatic activity of heterodimeric and monomeric PI3K $\gamma$  is significantly stimulated by G $\beta$  $\gamma$  (Stoyanov et al., 1995; Stephens et al., 1997; Tang and Downes, 1997; Leopoldt et al., 1998). However, when we challenged the concept in living cells, marked differences in the sensitivities between heterodimeric and monomeric PI3K $\gamma$  emerged. The G protein-coupled fMLP receptor activated p110 $\gamma$ /p101, but not p110 $\gamma$ , as evident from the translocation of fluorescent PtdIns-3,4,5-P<sub>3</sub> sensors or the stimulation of Akt phosphorylation. Likewise, coexpressed G $\beta$  $\gamma$  recruited p110 $\gamma$ /p101, but not p110 $\gamma$ , to membranes of HEK cells. Interestingly, PI3K $\beta$ , another G $\beta$  $\gamma$ -regulated PI3K, did not translocate to the membrane on GPCRs or G $\beta$  $\gamma$  stimulation, whereas RTKs induced membrane recruitment *in vivo* (unpublished data).

Does membrane recruitment of PI3K $\gamma$  by itself result in constitutive activation of p110 $\gamma$ ? To answer this intriguing question, we used an isoprenylated mutant of p110 $\gamma$ , i.e., p110 $\gamma$ -CAAX, which is permanently attached to the membrane, and thereby, is in close proximity to its lipid substrates. Expression of p110 $\gamma$ -CAAX only slightly enhanced membrane association of fluorescent PtdIns-3,4,5-P<sub>3</sub> sensors in HEK or VSM cells. Notably, it did not affect the morphology of HEK cells. In contrast, coexpression of G $\beta$  $\gamma$  together with p110 $\gamma$ -CAAX induced morphological changes comparable to cells transfected with plasmids encoding G $\beta$  $\gamma$  and p110 $\gamma$ /p101. Furthermore, stimulation of the cells with fMLP stimulated Akt phosphorylation and membrane recruitment of PH domains regardless of whether p110 $\gamma$ /p101 or p110 $\gamma$ -CAAX was the effector. This establishes a second role for G $\beta$  $\gamma$ , i.e., the activation of the membrane-attached catalytic p110 $\gamma$  subunit even in the absence of p101 (Fig. 9). Although G $\beta$  $\gamma$  interacts with either monomeric

**Figure 9. Hypothetical model for receptor-induced membrane recruitment and activation of heterodimeric PI3K $\gamma$ .** fMLP receptor, a prototypical heptahelical receptor coupled to G<sub>i</sub> proteins. PI3K $\gamma$ ; the cytosolic enzyme consists of a noncatalytic p101 subunit, which is in a tight complex with p110 $\gamma$ , thereby stabilizing p101. The NH<sub>2</sub> and COOH termini of p101 and p110 $\gamma$  are oriented in close proximity, respectively. Contact sites involve the NH<sub>2</sub> termini of both subunits. The modular domain structure of p110 $\gamma$  (RBD, Ras binding domain; C2, C2 domain; hel, helical domain; N-cat, C-cat, NH<sub>2</sub>- and COOH-terminal lobes of the catalytic domain) is based on the crystal structure of an NH<sub>2</sub>-terminally truncated p110 $\gamma$ .

(A) Membrane recruitment. The agonist-stimulated receptor induces the release of G $\beta$  $\gamma$  from G<sub>i</sub> proteins (dotted arrow). G $\beta$  $\gamma$  recruits the PI3K $\gamma$  heterodimer to the plasma membrane (dotted arrow) by binding to the noncatalytic p101 (hollow arrow). Accordingly, G $\beta$  $\gamma$  and p101 function as a membrane anchor and an adaptor for PI3K $\gamma$ , respectively. In addition, the C2 domain of p110 $\gamma$  may facilitate membrane attachment through interaction with phospholipids. p101 may also affect the interaction of PI3K $\gamma$  with the lipid interface. Membrane-attached PI3K $\gamma$  exhibits basal enzymatic activity. (B) Allosteric activation. At the membrane, G $\beta$  $\gamma$  activates PI3K $\gamma$  by direct interaction with p110 $\gamma$  (hollow arrows). This stimulation does not require p101. However, p101 may participate in G $\beta$  $\gamma$ -induced stimulation of membrane-attached p110 $\gamma$ . The stoichiometry of the G $\beta$  $\gamma$ -PI3K $\gamma$  interaction is unknown, i.e., G $\beta$  $\gamma$  may interact with p101 and p110 $\gamma$  through individual or common binding sites. G $\beta$  $\gamma$  binds to the NH<sub>2</sub>- and COOH-terminal part of p110 $\gamma$ , the latter harboring the catalytic domain. Thus, G $\beta$  $\gamma$  may allosterically activate PI3K $\gamma$  through a conformational change in the catalytic domain. Accordingly, G $\beta$  $\gamma$  significantly increases V<sub>max</sub> of PtdIns-3,4,5-P<sub>3</sub> production. PtdIns-3,4,5-P<sub>3</sub>, in turn, recruits PH domain-containing effectors such as GRP1 or Btk to the plasma membrane (dotted arrow).





PI3K $\gamma$  subunit through individual binding sites, it does not exclude the possibility that heterodimeric PI3K $\gamma$  forms either a common or different binding site(s) for G $\beta\gamma$ . Attempts to determine the stoichiometry of the interaction between heterodimeric PI3K $\gamma$  and one or more G $\beta\gamma$  were inconclusive. One possible reason may be a weak affinity between p110 $\gamma$  and G $\beta\gamma$ , whereas p101 binds at least with moderate affinity to G $\beta\gamma$  as determined by copurification studies (Stephens et al., 1997; Krugmann et al., 1999; Maier et al., 1999) and by a Biacore plasmon resonance approach (unpublished data).

In our paper, we present evidence that p110 $\gamma$  is stable as a monomer without p101, but not vice versa. This may explain why relevant amounts of native monomeric p101 do not occur in vivo (Wetzker, R., personal communication). p110 $\gamma$  can be expressed as a stable protein independent of the presence of p101, as shown previously (Fig. 2 C; Lopez-Illasaca et al., 1997, 1998; Leopoldt et al., 1998; Maier et al., 1999). Interestingly, the p110 subunit of class I<sub>A</sub> PI3Ks needs stabilization by forming a complex with the p85 adaptor (Yu et al., 1998). Accordingly, class I<sub>A</sub> p110 $\alpha,\beta,\delta$  subunits are thought to occur only in their adaptor-bound form. Moreover, the p85 adaptor is more abundant than the p110 counterparts (Ueki et al., 2002). In contrast, p110 $\gamma$  is also suggested to occur in the absence of p101 (Baier et al., 1999).

Increasing evidences suggest that monomeric p110 $\gamma$  may also function as a downstream regulator of GPCR-dependent signal transduction pathways in cells (Lopez-Illasaca et al., 1997, 1998; Bondeva et al., 1998; Murga et al., 1998; Baier et al., 1999). However, under in vivo conditions the p101 subunit seems mandatory for G protein-mediated activation of PI3K $\gamma$  by mediating membrane recruitment. Therefore, the question arises of how monomeric p110 $\gamma$  translocates to the membrane. In this context, recent in vitro evidence points to the possibility that membrane attachment of p110 $\gamma$  may involve binding to anionic phospholipids (Kirsch et al., 2001). In line with this finding, the majority of PI3K $\gamma$  is already associated with lipid vesicles in the absence of G $\beta\gamma$  under in vitro conditions, and vesicle-bound PI3K $\gamma$  can still be activated by G $\beta\gamma$  (Krugmann et al., 2002). Alternatively, p110 $\gamma$  may be recruited by binding to membrane-anchored proteins other than G $\beta\gamma$ . In this respect, p110 $\gamma$ , like all other class I PI3Ks, is directly activated by GTP-bound Ras (Pacold et al., 2000).

In conclusion, we present in vivo evidence that G $\beta\gamma$  may stimulate PI3K $\gamma$  in a dual and complementary way, i.e., by recruitment to the membrane, and by activation of the membrane-bound enzyme (Fig. 9). In this scenario, the p101 subunit functions as an adaptor molecule necessary to recruit the catalytic subunit to the plasma membrane through high affinity interaction with G $\beta\gamma$ . In turn, direct interaction between G $\beta\gamma$  and the membrane-attached catalytic p110 $\gamma$  subunit contributes to a final activation of the enzyme by a mechanism other than translocation.

## Materials and methods

### Construction of expression plasmids

For generation of expression plasmids of PI3K $\gamma$  subunits, restriction sites were introduced, and stop codons were removed by 8–12 cycles of PCR

using the indicated primers, a PCR system (Expand HF; Roche), and a pcDNA3.1/V5-His-TOPO vector (Invitrogen) for first subcloning. Subcloned PCR fragments were confirmed by sequencing with fluorescent dye terminators (ABI-Prism 377; PerkinElmer). Expression plasmids encoding NH<sub>2</sub>- and COOH-terminally tagged fusion proteins were generated by subsequent subcloning into the vectors pEYFP-C1 and pECFP-C1 (CLONTECH Laboratories, Inc.) or into pcDNA3-YFP and pcDNA3-CFP (Schaefer et al., 2001), respectively. The constructs are designated indicating the color and the position of the tag (see Fig. 1 A). In detail, wild-type p110 $\gamma$ ; human p110 $\gamma$  cDNA (Stoyanov et al., 1995; a corrected nucleotide sequence for p110 $\gamma$  is available from GenBank/EMBL/DBJ, accession no. AF327656) was amplified with the primers 5'-GCC ACC ATG GAG CTG GAG AAC TAT AA-3' and 5'-GGA TCC AGC TTT CAC AAT GTC TAT TG-3', and subcloned into pcDNA3 via KpnI and XhoI. p110 $\gamma$ -YFP and -CFP; the stop codon was replaced by an XbaI site using the primer 5'-GTC TAG AGC TGA ATG TTT CTC TCC CTT GT-3' and the same forward primer as above. Subcloning into pcDNA3-YFP and -CFP was done via BamHI and XbaI. YFP- and CFP-p110 $\gamma$ ; XhoI and BamHI sites were introduced using the primers 5'-CTC GAG GCA TGG AGC TGG AGA ACT A-3' and 5'-GGA TCC AGC TTT CAC AAT GTC TAT TG-3' for subcloning into pEYFP-C1 and pECFP-C1. p110 $\gamma$ -K833R; position 2498 was mutated from A to G using the QuikChange<sup>®</sup> Mutagenesis Kit (Stratagene) and appropriate primers. p110 $\gamma$ -CAAX; two Afel sites in p110 $\gamma$  were removed, and the stop codon was replaced by a new Afel site by silent mutations using the QuikChange<sup>®</sup> Mutagenesis Kit and appropriate primers. Adaptor oligonucleotides encoding the 18 COOH-terminal amino acids of H-Ras were inserted into the Afel and BamHI sites. Wild-type p101; the cDNA for porcine p101 (Stephens et al., 1997) was subcloned in pcDNA3 via EcoRI and NotI. An optimized ribosomal docking sequence was introduced by PCR using the primers 5'-GCC ACC ATG CAG CCA GGG GCC ACG GA-3' and 5'-GGC CCG AGA CGA AGG AGG T-3' and subsequent exchange of the 5'-end via HindIII and BsmBI. YFP- and CFP-p101; the EcoRI/NotI fragment of p101 was subcloned into EcoRI/Bsp120I-digested pEYFP-C1 or pECFP-C1. To adapt the reading frames, the HindIII site was blunted with Klenow fragment (New England Biolabs, Inc.) and religated. p101-YFP and -CFP; PCR with the primers 5'-GTC CTC TCC TCA CAC GGT TCT T-3' and 5'-GTC TAG AGG CAG AGC TCC GCT GAA AGT-3' generated the 3'-end of p101 with an XbaI site instead of the stop codon. To restore the full-length p101 cDNA, the 5'-part was excised from wild-type p101 in pcDNA3 with HindIII and ClaI (partial digest) and ligated to the HindIII/ClaI-digested 3'-end. Subsequent subcloning in pcDNA3-YFP and pcDNA3-CFP was done via HindIII and XbaI.

The human fMLP receptor cDNA (Boulay et al., 1990) was amplified with the primers 5'-GCC ACC ATG GAG ACA AAT TCC TCT CTC-3' and 5'-TCA CTT TGC CTG TAA CTC CAC-3' and subcloned in pcDNA3 via HindIII and XhoI. The cDNAs of G $\alpha_{12}$  (Conklin et al., 1993), human G $\beta_1$  (Codina et al., 1986), and bovine G $\gamma_2$  (Gautam et al., 1989) were subcloned into pcDNA3. Plasmids for GFP-GRP1<sub>PH</sub> and Ras N17 are described elsewhere (Ridley et al., 1992; Gray et al., 1999).

For generation of expression plasmids encoding CFP-tagged G $\beta_1$  and Btk<sub>PH</sub>, restriction sites were introduced by PCR using the indicated primers, the Advantage<sup>™</sup> II PCR enzyme system (CLONTECH Laboratories, Inc.) and the pGEM<sup>®</sup>-T Easy Vector (Promega) for first subcloning. The G $\beta_1$  cDNA was amplified using the primers 5'-TAC AAG TCC GGA CAA GCT TCC ATG AGT GAG CTT GAC CAG TTA CGG C-3' and 5'-CGG GAT CCG TCG ACC CAT GGT GGC GTT AGT TCC AGA TCT TGA GGA AGC-3', allowing for in-frame subcloning into the HindIII and BamHI sites of pECFP-C1. The cDNA encoding the PH domain of human Btk (Várnai et al., 1999) and adjacent 5' untranslated bases was amplified from cDNA of dibutyl-*c*-AMP-differentiated HL-60 cells using the primers 5'-CCA AGT CCT GGC ATC TCA ATG CAT CTG-3' and 5'-TGG AGA CTG GTG CTG CTG CTG GCT C-3'. A nested PCR was performed using the primers 5'-GGA AGA TCT CGA GCC ACC ATG GCC GCA GTG ATT CTG G-3' and 5'-GGG GAT CCC GGG CCC GAG GTT TTA AGC TTC CAT TCC TGT TCT CC-3', allowing for in-frame subcloning into the XhoI and BamHI sites of pECFP-N1 (CLONTECH Laboratories, Inc.). The cDNA inserts and flanking regions of the resulting CFP-G $\beta_1$  and Btk<sub>PH</sub>-CFP constructs were confirmed by sequencing.

### Cell culture, transfection, and intranuclear microinjection

HEK 293 cells (American Type Culture Collection) were grown at 37°C with 5% CO<sub>2</sub> in DME or in MEM with Earle's salts supplemented with 10% FCS, 100  $\mu$ g/ml streptomycin, and 100 U/ml penicillin. All transfections were done with a FuGENE<sup>™</sup> 6 transfection reagent (Roche) following the manufacturer's recommendations. For fluorescence microscopy experiments, cells were seeded on glass coverslips. For confocal imaging of the

subcellular localization of the PI3K $\gamma$  subunits, cells were transfected with 0.1  $\mu$ g of plasmid encoding YFP-tagged PI3K $\gamma$  subunits, 0.2  $\mu$ g of plasmid for the untagged complementary subunit, and 1  $\mu$ g each of plasmid for G $\beta_1$  and G $\gamma_2$  (except for the experiment shown in Fig. 4 B; 0.1  $\mu$ g YFP-p101 + 2  $\mu$ g G $\beta_1$  or G $\gamma_2$  alone, or 0.5  $\mu$ g G $\beta_1$  + 0.5  $\mu$ g G $\gamma_2$  + 1  $\mu$ g G $\alpha_{12}$ ). For monitoring PH domain translocation, or Akt- or ERK phosphorylation, HEK cells were transfected with 0.2  $\mu$ g plasmid encoding the fMLP receptor, and 0.4  $\mu$ g each of the plasmids encoding the PI3K $\gamma$  subunits and the fluorescent PH domain. The total amount of transfected cDNA was always kept constant (2.5  $\mu$ g/well) by the addition of empty expression vector. For FRET analysis, cells were transfected with 1.5  $\mu$ g of plasmid encoding the YFP-tagged p110 $\gamma$  and 0.5  $\mu$ g of plasmid for CFP-tagged p101. All experiments were performed one or two days after transfection.

VSM cells from neonatal rat aortas were cultured as described previously (Reusch et al., 2001). Cells were seeded on glass coverslips and microinjected with the plasmids for GFP-GRP1<sub>PH</sub> (0.4  $\mu$ g/ml), fMLP receptor (0.05  $\mu$ g/ml), p110 $\gamma$  (0.05  $\mu$ g/ml), and p101 (0.05  $\mu$ g/ml) using an Eppendorf micromanipulator and transjector. Confocal images were taken one day after microinjection.

### Immunoblot analysis of whole-cell lysates, gel filtration, and membrane fractions

p110 $\gamma$ /p101 titration; transfected HEK cells were lysed in Laemmli buffer and whole-cell lysates including nuclei were subjected to a 10% SDS-PAGE. Proteins were blotted on nitrocellulose membranes, probed with anti-GFP (CLONTECH Laboratories, Inc.) and peroxidase-coupled anti-rabbit IgG antibodies (Sigma-Aldrich) and visualized by ECL (Amersham Biosciences). Akt and ERK phosphorylation; HEK 293 cells were transfected as indicated with the plasmids encoding the fMLP receptor (0.2  $\mu$ g), PI3K $\gamma$  subunits (each 0.4  $\mu$ g), and H-Ras N17 (1.5  $\mu$ g). Cells were serum-starved overnight, then stimulated as indicated, and lysed in Laemmli buffer. Whole-cell lysates were subjected to SDS-PAGE and immunoblotting, and probed with anti-Phospho-Akt or anti-Phospho-ERK1/2 and anti-ERK1/2 as described previously (Reusch et al., 2001). Gel filtration; HEK cells were transfected with equal amounts of the plasmids for YFP-p110 $\gamma$  (or p110 $\gamma$ -YFP) and CFP-p101 (or pcDNA3). Cells were washed in PBS and lysed in 20 mM Hepes, pH 7.5, 150 mM NaCl, 10 mM  $\beta$ -mercaptoethanol, 4 mM EDTA, 0.2% polyoxyethylene-10-lauryl ether (C<sub>12</sub>E<sub>10</sub>), 200  $\mu$ M Pefabloc<sup>®</sup> SC, 30  $\mu$ g/ml TPCK, 30  $\mu$ g/ml trypsin inhibitor, and 50  $\mu$ g/ml benzamide by repetitive aspiration through a 26-gauge needle. Cytosols were prepared (100,000 g for 30 min at 4°C), and subjected to gel filtration on a 24-ml Superdex 200 column and eluted with the same buffer on an ÄKTA<sup>™</sup> purifier system (Amersham Biosciences). Fractions were collected, and aliquots were subjected to SDS-PAGE and immunoblotting with anti-GFP. Preparation of membrane fractions; HEK cells were transfected as indicated with the plasmids for YFP-p110 $\gamma$ -K833R (0.1  $\mu$ g), p101 (0.2  $\mu$ g), G $\beta_1$  (1.0  $\mu$ g), and G $\gamma_2$  (1.0  $\mu$ g). Cells were washed with PBS and lysed in PBS with protease inhibitors (see above) by repetitive aspiration through a 26-gauge needle. Membranes were prepared (16,000 g for 20 min at 4°C), redissolved in Laemmli buffer, subjected to SDS-PAGE and immunoblotting, and probed with anti-p110 $\gamma$  (see next section) and anti-G $\beta_{\text{common}}$  (AS398; Leopoldt et al., 1997).

### In vitro PI3K assay

HEK cells were transfected with equal amounts of the plasmids encoding p110 $\gamma$  and p101 (or empty pcDNA3 to keep the total amount of transfected cDNA constant). Cell lysates were subjected to immunoprecipitation using a monoclonal anti-p110 $\gamma$  antibody (Bondev et al., 2001). In brief, protein A Sepharose was preincubated with or without antibody, washed, incubated overnight with cleared lysates, and washed again. The in vitro PI3K assay was performed as described previously (Maier et al., 1999). Radioactive PtdIns-3,4,5-P<sub>3</sub> was visualized with a PhosphorImager (Fuji Bas-Reader 1500; Ray Test).

### Fluorescence imaging and detection of FRET

Glass coverslips were mounted on a custom-made chamber and covered with a Hepes-buffered solution containing 138 mM NaCl, 6 mM KCl, 1 mM MgCl<sub>2</sub>, 1 mM CaCl<sub>2</sub>, 5.5 mM glucose, 10 mM Hepes, pH 7.5, and 2 mg/ml BSA. For confocal imaging, an inverted confocal laser scanning microscope with a Plan-Apochromat 63 $\times$ /1.4 objective (model LSM 510; Carl Zeiss MicroImaging, Inc.) was used. YFP or GFP were excited at 488 nm, and fluorescence emission was detected through a 505-nm long pass filter. CFP was excited 458 nm, and detected through a 475-nm long pass filter. Pinholes were adjusted to yield optical sections of 0.5–1.5  $\mu$ m.

FRET analysis was performed using an inverted microscope with a Plan-Apochromat 63 $\times$ /1.4 objective (Axiovert 100; Carl Zeiss MicroImaging,

Inc.). CFP and YFP were alternately excited at 440 and 500 nm with a monochromator (Polychrome II; TILL Photonics) in combination with a dual reflectivity dichroic mirror (<460 nm and 500–520 nm; Chroma Technology Corp.). Emitted light was filtered through 475–505-nm (CFP) and 535–565-nm (YFP) band pass filters, changed by a motorized filter wheel (Lambda 10/2; Sutter Instrument Co.), and detected by a cooled CCD camera (Imago; TILL Photonics). FRET was assessed as recovery of CFP (donor) fluorescence during YFP (acceptor) bleach. First, CFP and YFP fluorescences without acceptor bleach were recorded during 30 cycles with a 10–20-ms exposure. Then, 60 cycles were recorded with an additional 2-s illumination per cycle at 510 nm to bleach YFP.

Thanks to Claudia Plum, A. Schulz and J. Malkewitz for technical assistance. We are grateful to Drs. P. Gierschik, A. Gray and P. Downes, M.I. Simon, L. Stephens and P. Hawkins, and R. Wetzker for providing experimental tools. Thanks to Celsa Antao-Paetsch for assistance in preparation of the manuscript. We appreciate valuable discussions with Drs. Len Stephens, Phil Hawkins, Lewis Cantley, Reinhard Wetzker, and Roland Piekorz.

This work was supported by the Deutsche Forschungsgemeinschaft and Fonds der Chemischen Industrie.

Submitted: 21 October 2002

Revised: 2 December 2002

Accepted: 2 December 2002

## References

- Al-Aoukaty, A., B. Rolstad, and A.A. Maghazachi. 1999. Recruitment of pleckstrin and phosphoinositide 3-kinase  $\gamma$  into the cell membranes, and their association with G $\beta\gamma$  after activation of NK cells with chemokines. *J. Immunol.* 162:3249–3255.
- Balla, T., T. Bondeva, and P. Várnai. 2000. How accurately can we image inositol lipids in living cells? *Trends Pharmacol. Sci.* 21:238–241.
- Baier, R., T. Bondeva, R. Klinger, A. Bondev, and R. Wetzker. 1999. Retinoic acid induces selective expression of phosphoinositide 3-kinase  $\gamma$  in myelomonocytic U937 cells. *Cell Growth Differ.* 10:447–456.
- Bondev, A., T. Bondeva, and R. Wetzker. 2001. Regulation of phosphoinositide 3-kinase  $\gamma$  protein kinase activity *in vitro* and in COS-7 cells. *Signal Transduction.* 1:79–85.
- Bondeva, T., L. Pirola, G. Bulgarelli-Leva, I. Rubio, R. Wetzker, and M.P. Wyman. 1998. Bifurcation of lipid and protein kinase signals of PI3K $\gamma$  to the protein kinases PKB and MAPK. *Science.* 282:293–296.
- Boulay, F., M. Tardif, L. Bouchon, and P. Vignais. 1990. The human N-formylpeptide receptor. Characterization of two cDNA isolates and evidence for a new subfamily of G-protein-coupled receptors. *Biochemistry.* 29:11123–11133.
- Cantley, L.C. 2002. The phosphoinositide 3-kinase pathway. *Science.* 296:1655–1657.
- Codina, J., D. Stengel, S.L. Woo, and L. Birnbaumer. 1986.  $\beta$ -subunits of the human liver G $_i$ /G $_o$  signal-transducing proteins and those of bovine retinal rod cell transducin are identical. *FEBS Lett.* 207:187–192.
- Conklin, B.R., Z. Farfel, K.D. Lustig, D. Julius, and H.R. Bourne. 1993. Substitution of 3 amino acids switches receptor specificity of G $_q\alpha$  to that of G $_i\alpha$ . *Nature.* 363:274–276.
- Fruman, D.A., R.E. Meyers, and L.C. Cantley. 1998. Phosphoinositide kinases. *Annu. Rev. Biochem.* 67:481–507.
- Gautam, N., M. Baetscher, R. Aebersold, and M.I. Simon. 1989. A G protein  $\gamma$  subunit shares homology with ras proteins. *Science.* 244:971–974.
- Gillham, H., M.C. Golding, R. Pepperkok, and W.J. Gullick. 1999. Intracellular movement of green fluorescent protein-tagged phosphatidylinositol 3-kinase in response to growth factor receptor signaling. *J. Cell Biol.* 146:869–880.
- Gray, A., J. Van Der Kaay, and C.P. Downes. 1999. The pleckstrin homology domains of protein kinase B and GRP1 (general receptor for phosphoinositides-1) are sensitive and selective probes for the cellular detection of phosphatidylinositol 3,4-bisphosphate and/or phosphatidylinositol 3,4,5-trisphosphate *in vivo*. *Biochem. J.* 344:929–936.
- Hurley, J.H., and S. Misra. 2000. Signaling and subcellular targeting by membrane-binding domains. *Annu. Rev. Biophys. Biomol. Struct.* 29:49–79.
- Katso, R., K. Okkenhaug, K. Ahmadi, S. White, J. Timms, and M.D. Waterfield. 2001. Cellular function of phosphoinositide 3-kinases: implications for development, homeostasis, and cancer. *Annu. Rev. Cell Dev. Biol.* 17:615–675.
- Kirsch, C., R. Wetzker, and R. Klinger. 2001. Anionic phospholipids are involved in membrane targeting of PI3-kinase  $\gamma$ . *Biochem. Biophys. Res. Commun.* 282:691–696.

- Klippel, A., C. Reinhard, W.M. Kavanaugh, G. Apell, M.A. Escobedo, and L.T. Williams. 1996. Membrane localization of phosphatidylinositol 3-kinase is sufficient to activate multiple signal-transducing kinase pathways. *Mol. Cell Biol.* 16:4117–4127.
- Krugmann, S., P.T. Hawkins, N. Pryer, and S. Braselmann. 1999. Characterizing the interactions between the two subunits of the p101/p110 $\gamma$  phosphoinositide 3-kinase and their role in the activation of this enzyme by G $\beta\gamma$  subunits. *J. Biol. Chem.* 274:17152–17158.
- Krugmann, S., M.A. Cooper, D.H. Williams, P.T. Hawkins, and L.R. Stephens. 2002. Mechanism of the regulation of type I $\beta$  phosphoinositide 3OH-kinase by G-protein  $\beta\gamma$  subunits. *Biochem. J.* 362:725–731.
- Kurosu, H., T. Maehama, T. Okada, T. Yamamoto, S. Hoshino, Y. Fukui, M. Ui, O. Hazeki, and T. Katada. 1997. Heterodimeric phosphoinositide 3-kinase consisting of p85 and p110 $\beta$  is synergistically activated by the  $\beta\gamma$  subunits of G proteins and phosphotyrosyl peptide. *J. Biol. Chem.* 272:24252–24256.
- Leopoldt, D., C. Harteneck, and B. Nürnberg. 1997. G proteins endogenously expressed in Sf9 cells: interactions with mammalian histamine receptors *Nawyn Schmiedebergs Arch. Pharmacol.* 356:216–224.
- Leopoldt, D., T. Hanck, T. Exner, U. Maier, R. Wetzker, and B. Nürnberg. 1998. G $\beta\gamma$  stimulates phosphoinositide 3-kinase- $\gamma$  by direct interaction with two domains of the catalytic p110 subunit. *J. Biol. Chem.* 273:7024–7029.
- Lietzke, S.E., S. Bose, T. Cronin, J. Klarlund, A. Chawla, M.P. Czech, and D.G. Lambright. 2000. Structural basis of 3-phosphoinositide recognition by pleckstrin homology domains. *Mol. Cell.* 6:385–394.
- Lopez-Illasaca, M., P. Crespo, P.G. Pellici, J.S. Gutkind, and R. Wetzker. 1997. Linkage of G protein-coupled receptors to the MAPK signaling pathway through PI3-kinase  $\gamma$ . *Science.* 275:394–397.
- Lopez-Illasaca, M., J.S. Gutkind, and R. Wetzker. 1998. Phosphoinositide 3-kinase  $\gamma$  is a mediator of G $\beta\gamma$ -dependent Jun kinase activation. *J. Biol. Chem.* 273:2505–2508.
- Maier, U., A. Babich, and B. Nürnberg. 1999. Roles of non-catalytic subunits in G $\beta\gamma$ -induced activation of class I phosphoinositide 3-kinase isoforms  $\beta$  and  $\gamma$ . *J. Biol. Chem.* 274:29311–29317.
- Maier, U., A. Babich, N. Macrez, D. Leopoldt, P. Gierschik, D. Illenberger, and B. Nürnberg. 2000. G $\beta_5\gamma_2$  is a highly selective activator of phospholipid-dependent enzymes. *J. Biol. Chem.* 275:13746–13754.
- Metjian, A., R.L. Roll, A.D. Ma, and C.S. Abrams. 1999. Agonists cause nuclear translocation of phosphatidylinositol 3-kinase  $\gamma$ . A G $\beta\gamma$ -dependent pathway that requires the p110 $\gamma$  amino terminus. *J. Biol. Chem.* 274:27943–27947.
- Murga, C., L. Laguigne, R. Wetzker, A. Cuadrado, and J.S. Gutkind. 1998. Activation of Akt/protein kinase B by G protein-coupled receptors. A role for  $\alpha$  and  $\beta\gamma$  subunits of heterotrimeric G proteins acting through phosphatidylinositol-3-OH kinase  $\gamma$ . *J. Biol. Chem.* 273:19080–19085.
- Naccache, P.H., S. Levasseur, G. Lachance, S. Chakravarti, S.G. Bourgoin, and S.R. McColl. 2000. Stimulation of human neutrophils by chemotactic factors is associated with the activation of phosphatidylinositol 3-kinase  $\gamma$ . *J. Biol. Chem.* 275:23636–23641.
- Pacold, M.E., S. Suire, O. Perisic, S. Lara-Gonzalez, C.T. Davis, E.H. Walker, P.T. Hawkins, L. Stephens, J.F. Eccleston, and R.L. Williams. 2000. Crystal structure and functional analysis of Ras binding to its effector phosphoinositide 3-kinase  $\gamma$ . *Cell.* 103:931–943.
- Reusch, H.P., M. Schaefer, C. Plum, G. Schultz, and M. Paul. 2001. G $\beta\gamma$  mediate differentiation of vascular smooth muscle cells. *J. Biol. Chem.* 276:19540–19547.
- Ridley, A.J., H.F. Paterson, C.L. Johnston, D. Diekmann, and A. Hall. 1992. The small GTP-binding protein rac regulates growth factor-induced membrane ruffling. *Cell.* 7:401–410.
- Schaefer, M., N. Albrecht, T. Hofmann, T. Gudermann, and G. Schultz. 2001. Diffusion-limited translocation mechanism of protein kinase C isotypes. *FASEB J.* 15:1634–1636.
- Simonsen, A., A.E. Wurmser, S.D. Emr, and H. Stenmark. 2001. The role of phosphoinositides in membrane transport. *Curr. Opin. Cell Biol.* 13:485–492.
- Stephens, L.R., T.R. Jackson, and P.T. Hawkins. 1993. Agonist-stimulated synthesis of phosphatidylinositol(3,4,5)-trisphosphate: a new intracellular signaling system? *Biochim. Biophys. Acta.* 1179:27–75.
- Stephens, L., A. Smrcka, F.T. Cooke, T.R. Jackson, P.C. Sternweis, and P.T. Hawkins. 1994. A novel phosphoinositide 3 kinase activity in myeloid-derived cells is activated by G protein  $\beta\gamma$  subunits. *Cell.* 77:83–93.
- Stephens, L.R., A. Eguinoa, H. Erdjument-Bromage, M. Lui, F. Cooke, J. Coadwell, A.S. Smrcka, M. Thelen, K. Cadwallader, P. Tempst, and P.T. Hawkins. 1997. The G $\beta\gamma$  sensitivity of a PI3K is dependent upon a tightly associated adaptor, p101. *Cell.* 89:105–114.
- Stoyanov, B., S. Volinia, T. Hanck, I. Rubio, M. Loubtchenkov, D. Malek, S. Stoyanova, B. Vanhaesebroeck, R. Dhand, B. Nürnberg, et al. 1995. Cloning and characterization of a G protein-activated human phosphoinositide-3 kinase. *Science.* 269:690–693.
- Tang, X., and C.P. Downes. 1997. Purification and characterization of G $\beta\gamma$ -responsive phosphoinositide 3-kinases from pig platelet cytosol. *J. Biol. Chem.* 272:14193–14199.
- Teruel, M.N., and T. Meyer. 2000. Translocation and reversible localization of signaling proteins: a dynamic future for signal transduction. *Cell.* 103:181–184.
- Ueki, K., D.A. Fruman, S.M. Brachmann, Y.H. Tseng, L.C. Cantley, and C.R. Kahn. 2002. Molecular balance between the regulatory and catalytic subunits of phosphoinositide 3-kinase regulates cell signaling and survival. *Mol. Cell Biol.* 22:965–977.
- Vanhaesebroeck, B., S.J. Leevers, K. Ahmadi, J. Timms, R. Katso, P.C. Driscoll, R. Woscholski, P.J. Parker, and M.D. Waterfield. 2001. Synthesis and function of 3-phosphorylated inositol lipids. *Annu. Rev. Biochem.* 70:535–602.
- Várnai, P., K.I. Rother, and T. Balla. 1999. Phosphatidylinositol 3-kinase-dependent membrane association of the Bruton's tyrosine kinase pleckstrin homology domain visualized in single living cells. *J. Biol. Chem.* 274:10983–10989.
- Walker, E.H., O. Perisic, C. Ried, L. Stephens, and R.L. Williams. 1999. Structural insights into phosphoinositide 3-kinase catalysis and signalling. *Nature.* 402:313–320.
- Wishart, M.J., G.S. Taylor, and J.E. Dixon. 2001. Phoxy lipids: Revealing PX domains as phosphoinositide binding modules. *Cell.* 105:817–820.
- Yu, J., Y. Zhang, J. McIlroy, T. Rordorf-Nikoloic, G.A. Orr, and J.M. Backer. 1998. Regulation of the p85/p110 phosphatidylinositol 3'-kinase: stabilization and inhibition of the p110 $\alpha$  catalytic subunit by the p85 regulatory subunit. *Mol. Cell Biol.* 18:1379–1387.